tvst
Article

The Effect of Age-Related Macular Degeneration on Polarization Pattern Perception

Gary P. Misson[1,2], Stephen J. Anderson[1], Richard A. Armstrong[1], Mark Gilett[2], and David Reynolds[2]

[1] School of Optometry, College of Life and Health Sciences, Aston University, Birmingham, UK
[2] Department of Ophthalmology, South Warwickshire NHS Foundation Trust, Lakin Road, Warwick, UK

Correspondence: Gary P. Misson, Department of Ophthalmology, South Warwickshire NHS Foundation Trust, Lakin Road, Warwick, CV34 5BW, UK.
e-mail: g.misson@aston.ac.uk

Received: March 15, 2021
Accepted: July 19, 2021
Published: August 5, 2021

Keywords: polarized light; vision; haidinger's brushes; macula; macular pigment

Citation: Misson GP, Anderson SJ, Armstrong RA, Gilett M, Reynolds D. The effect of age-related macular degeneration on polarization pattern perception. Transl Vis Sci Technol. 2021;10(9):8, https://doi.org/10.1167/tvst.10.9.8

Purpose: The purpose of this study was to determine if a battery of polarization-modulated stimuli, quantified as a single metric, is effective in identifying macular disease in the presence/absence of cataract or pseudophakia.

Methods: Using a modified liquid crystal display, polarization pattern perception (PPP) for a formulated battery of geometric and logMAR stimuli was evaluated in participants that had either no eye pathology (healthy participants) or were grouped according to the presence of cataract, pseudophakia, and/or age-related macular degeneration (AMD). PPP was quantified as response frequencies to individual stimuli, and as a novel monocular polarization sensitivity score (*Ps*) based on perception of the stimulus battery set.

Results: Stimulus response frequencies were pattern-dependent and, compared with healthy participants, reduced for cataract and AMD groups but not for subjects with pseudophakia. Compared with healthy eyes ($n = 47$, median $Ps = 17$), *Ps* was significantly reduced by AMD ($n = 59$, median $Ps = 1$, $P < 0.001$) and, to a lesser extent, by cataracts ($n = 80$, median $Ps = 6$, $P < 0.001$). There was no significant difference between *Ps* for healthy and pseudophakic eyes ($n = 47$, median $Ps = 13$, $P = 0.323$). There was no significant correlation between *Ps* and logMAR visual acuity.

Conclusions: In the absence of significant cataract, or in pseudophakia, a set of polarization-modulated visual stimuli, quantified as the *Ps* score, distinguishes AMD from healthy maculae.

Translational Relevance: Perception of polarization-modulated stimuli, previously shown to be macula-dependent in a laboratory setting, is effective as a test of macular function in health and disease in a clinic setting.

Introduction

Humans can perceive and identify structured visual stimuli defined only by their state of polarization,[1–3] an ability that has been termed polarization pattern perception (PPP). Contrary to previous assumptions, evidence based on PPP suggests that humans are capable of a high degree of polarization sensitivity, being able to detect differences in angle of polarization as little as 5 degrees and differences in degrees of polarization of 25% or less.

As with the related phenomenon of Haidinger's brush (HB),[4–7] PPP is dependent on: (i) the ocular media transmitting linear polarized light without significant modification; (ii) the structural integrity of the fovea; and (iii) the presence of macular pigment. Any ocular disorder affecting one or more of these factors may interfere with polarization perception. This is known for HB, where the perception of the phenomenon is reduced or abolished by disorders of the retina and macula,[8–10] and/or by low levels of macular pigment.[11]

Refractive error and media opacities have little effect on the visibility of HB,[9,12] the perception of which has been proposed as a prognostic indicator for cataract surgery.[12] However, the detection of HB is relatively nonspecific with respect to different eye

conditions.[10] Furthermore, the quantification of polarization perception based on HB alone is limited by the spatiotemporal characteristics of this single percept. Other drawbacks to the use of HB in clinical practice include the difficulty with which the phenomenon is perceived, the tendency of the static percept to fade rapidly, and the cumbersome electromechanical apparatus required for its generation.

Our methodology for determining polarization pattern perception overcomes the disadvantages of previous clinical applications of HB in several ways. First, polarization-modulated patterned stimuli are easily generated by inexpensive, compact, solid-state technology. Second, in addition to qualitative assessments, quantitative polarization perceptual measures can be obtained using sets of polarization-modulated patterns that can be graded according to salience. Third, polarization pattern stimuli are easier to discern and describe than the peculiarities of HB.

Previous studies of human polarization perception typically used established psychophysical stimuli (e.g. gratings) or Landolt-C configurations, and employed trained observers.[2,3] The stimuli of the present study were developed for naïve observers in a clinic setting, and were designed to provide a stimulus set of graded salience that yielded a robust quantification of polarization pattern perception. The stimuli included those successfully used in previous psychophysical and electrophysiological investigations of human vision (e.g. gratings and checkerboard patterns), novel geometric patterns whose spatial discontinuities/sharp edges complemented the underlying radial nature of macular architecture and optotypes.

In a previous report,[13] we demonstrated a graded set of stimuli that were appropriate to assess the full extent of polarization perception in normally sighted individuals, and that normal sensitivity measures were reduced in a heterogeneous set of individuals with clinically unhealthy eyes. Our principal goal in this study was to determine whether polarization-modulated stimuli are effective in distinguishing individuals with macular disease, as represented by age-related macular degeneration (AMD), from individuals with healthy maculae. To do so, we assessed individuals diagnosed with two eye disorders (AMD and/or cataract) and one surgical intervention (cataract surgery). The reasons for choosing these particular eye conditions are: (i) all are common in individuals over 65 years of age; (ii) AMD and cataract frequently co-exist, so the effect of each and both combined on PPP must be understood if the latter is to be of diagnostic value; (iii) intraocular lens implants made of polymer materials could potentially alter the polarization state of transmitted light, again interfering with the diagnostic value of PPP.

Available data for the patient demographic described above indicates that, whereas cataracts and AMD co-exist in many individuals (10% of individuals undergoing cataract surgery have co-existing AMD, Day et al. 2015), the majority of individuals with AMD will either have visually insignificant cataracts or will be pseudophakic. Furthermore, the possible acceleration of AMD following cataract surgery (e.g. Beaver Dam study[14]), although disputed,[15] emphasizes the importance of postsurgical macular function assessment and monitoring.

A novel metric of polarization pattern perception, based on the weighted sum of the polarization responses to each pattern/optotype, was used to derive a polarization sensitivity score (*Ps*), which was used to compare polarization pattern responses in the clinically defined categories. In particular, we sought to determine: (i) whether a quantifiable polarization-modulated stimulus set, generated with existing LCD technology, is effective in distinguishing AMD from healthy maculae; (ii) the effects of pseudophakia on PPP; and (iii) if, as with HB, cataractous media opacities have little effect on PPP.

Methods

The study was a nonrandomized, retrospective consecutive case series, assessing clinical data of staff and adult patients from the Machen Eye Unit of Warwick Hospital, South Warwickshire NHS foundation Trust, UK, between November 2017 and April 2019. The study adhered to the tenets of the Declaration of Helsinki, and was approved by the National Health Service Health Research Authority (IRAS project ID 224715) following Research Ethics Committee approval (REC reference 17/WA/0180). All participants gave informed consent following explanation of the nature of the study.

Participant Characteristics

Of the 221 participants (data summary in Supplementary Material Table S1), 21 had no manifest pathology in either eye (healthy group). The patient group comprised 200 individuals who, in one or both eyes, were normophakic, pseudophakic, or had cataract, and either had AMD or clinically healthy fundi. Cataracts were defined as any symptomatic lens opacification identifiable on slit-lamp examination. AMD was defined by an Age-Related Eye Disease Study (AREDS) grading of two or greater.[16]

Table 1. Eye Diagnostic Categories (332 Eyes of 221 Participants), Grouped According to the Presence or Absence of Cataract or Pseudophakia

		Normophakia	Cataract	Pseudophakia
No AMD	*n*	47	80	47
Sex	M	17	29	24
	F	30	51	23
Eye	R	23	42	20
	L	24	38	27
Age	Mean	71.1	74.1	73.7
	SD	7.1	11.4	10.8
	Max	90.9	92.2	86.8
	Min	60.2	36.2	47.5
AMD present	*n*	59	42	57
Sex	M	22	15	13
	F	37	27	44
Eye	R	27	21	27
	L	32	21	30
Age	Mean	77.9	83.0	83.8
	SD	6.8	4.1	6.8
	Max	91.9	89.6	96.4
	Min	65.5	71.8	70.2

All healthy participants were over 60 years of age, chosen randomly from a large database to affect a group-mean age within one decade of the patient group. Individuals with single or multiple pathologies – other than cataract, pseudophakia, or AMD – were excluded from the study, as were data from eyes with visual acuities worse than 1.2 logMAR.

The healthy-eye diagnostic group comprised healthy-eye data from the patient group combined with data of one eye (randomly chosen) from each individual in the healthy group ($n = 47$; normophakia / no AMD; Table 1). The unhealthy-eye diagnostic groups (see Table 1) comprised data from one or both eyes of normophakic individuals with AMD, and those with cataract or pseudophakia in the presence or absence of AMD. Different uniocular pathologies and asymmetry of bilateral pathology justified the separate analysis of eye pairs.

All patients with pseudophakia had uneventful cataract surgery at least 4 months prior to testing. Of the 140 pseudophakic eyes, 63 had TECNIS iTEC PCB00 intraocular lenses (range = 6–34D, mean = 22.3, SD = 4.3), and 35 had Alcon AcrySof MA60AC intraocular lenses (range = 13–27.5, mean = 22.2, SD = 2.6). The intraocular lens data of 42 eyes were unknown.

Data Acquisition and Quantification

Corrected distance visual acuity was measured using a standard Bailey-Lovie (early treatment diabetic retinopathy study [ETDRS]) chart, and recorded as a logMAR value. Optical coherence tomography (OCT) was performed using a Topcon DRI OCT Triton Plus swept source system. Allocation to diagnostic categories was based on clinical assessment, including slit-lamp examination, dilated fundoscopy, and OCT.

PPP was assessed using hardware and methodology detailed elsewhere.[13] In brief, participants were asked to identify images presented on a polarization stimulus generator that consisted of a liquid crystal display (Asus VS278H from ASUSTeK Computer Inc, Taiwan) from which the front polarizer had been removed.[1–3,17] The screen emitted a constant polarization-independent luminance of 8.0 cd m^{-2} with a peak wavelength 460 nm, and subtended visual angles of 11 degrees (width) by 6.5 degrees (height) at an observation distance of 3 m. Polarization output was calibrated as described elsewhere,[3] and confirmed to be predominantly linearly polarized (degree of linear polarization = 0.94). Polarization **E**-vector axes, measured anticlockwise from the horizontal, varied from 54 degrees for greyscale 000 (foreground of stimulus images) to 147 degrees for greyscale 255 (stimulus background).

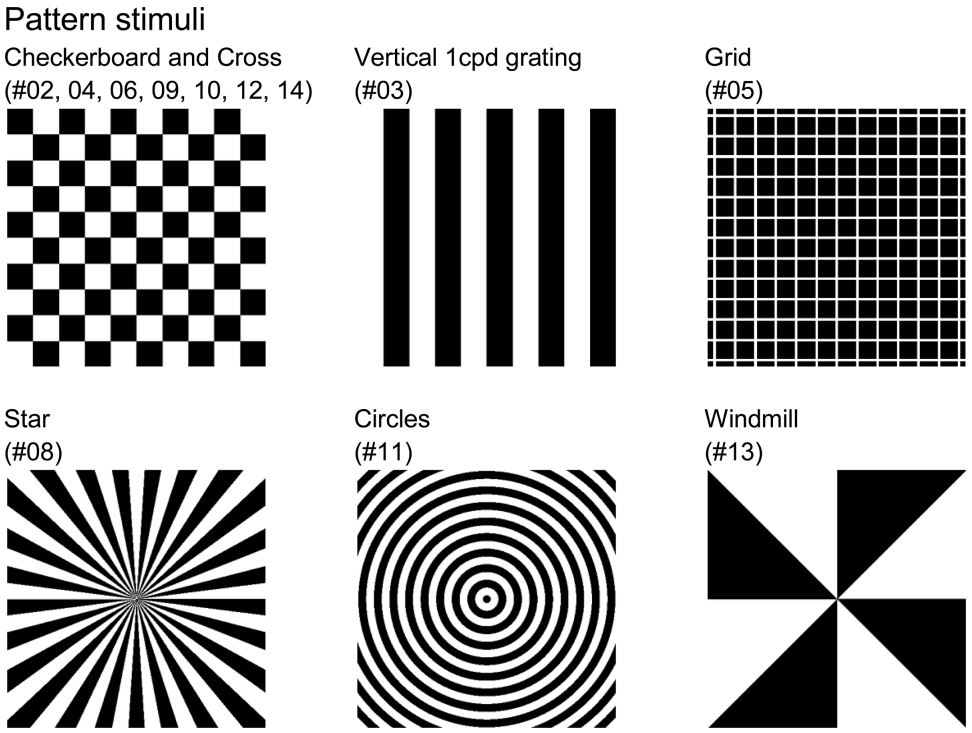

Figure 1. Polarization pattern stimuli. The six types of pattern stimuli are shown with their descriptors and stimulus number. Checkerboard stimuli had the following fundamental spatial frequencies: #02, 1 cpd; #04, 2 cpd; #06, 6 cpd; #09, 12 cpd; #12, 4cpd; #14, 9 cpd. Stimulus #10 is a 0.25 cpd checkerboard, which gives a cross-like percept. The alternating (#01) and static (#07) uniform field Haidinger's brush stimuli are omitted, as are the optotypes.

Ametropic participants were corrected for the 3 m working distance using optically isotropic (stress-free) glass lenses mounted in a trial frame. All testing was monocular. Each eye of a participant was assessed in turn by one of two trained ophthalmic technicians, both of whom were unaware of the participant's clinical details. Before testing, the technician explained the task and the expected appearance of the stimuli according to a set preamble. Typical run-times for the full series of slides were between 5 and 10 minutes per eye.

The stimulus set consisted of uniform fields, geometric patterns and optotypes (Fig. 1).[13] The uniform field stimuli comprised either: (i) a blank screen with a grey scale of constant 000 (foreground "black," angle of polarization 54 degrees) to give a static HB percept, or (ii) a greyscale 000 alternating with 255 (background "white," angle of polarization 147 degrees) at 1 Hz to give an alternating (dynamic) HB percept. Pattern stimuli, composed of foreground and background polarization states, consisted of one of six geometric patterns (see Fig. 1). The checkerboard was presented either as a pattern-reversing 1 cycle per degree (cpd) image, or as a static image with a fundamental spatial frequency of 0.25, 2, 4, 6, 9, or 12 cpd. Standard Sloan optotypes were presented in random order of five optotypes per screen of a particular logMAR value. The range covered was logMAR 0.3–1.2 in 0.1 increments.

Two response criteria for polarization pattern sensitivity were used. First, pattern/optotype identification, defined as the ability to identify accurately the stimulus pattern/optotype. Second, pattern detection, defined as the ability to detect but not identify the presence of a pattern.

For the second part of the study, the collected responses from an individual to the polarization stimulus set was represented as a single metric quantifying that individual's ability to perceive polarization stimuli. The polarization sensitivity (*Ps*) score metric devised for the present study was the weighted sum of scores of the stimulus set response for individual participants. The *Ps* score was based on previous findings,[13] and relates to the relative sensitivity of the criteria of detection and identification of stimuli. A score of 2 was given for the correct identification of each of the 14 geometric or 35 optotype stimuli; a score of one was given for each detection (without identification) of a pattern stimulus; a score of zero was given

for the inability to detect a pattern stimulus from its background, or incorrect optotype identification. The maximum possible *Ps* score per eye was 98.

Statistical Methods

Conventional parametric and nonparametric analyses were used where appropriate. The nonparametric methods used for analysis of *Ps* scores included Kruskal-Wallace test of ranks and the Mann-Whitney *U* test for comparison of two independent samples.

Multiple 2 × 2 contingency tables were analyzed using the Cochran-Mantel-Haenszel Test and Woolf's test for heterogeneity of odds ratios (ORs). As previously studied,[13] the OR was interpreted as the amount by which the ratio of positive to negative responses for a particular group has to be multiplied by to equal the ratio of positive to negative responses for the healthy group.

Receiver operating characteristic (ROC) curves and area under the ROC curve (AUROC) were used to determine the diagnostic ability of the clinical group classificatory variable as the *Ps* discriminatory threshold varied.

Data were managed using Microsoft Access and Microsoft Excel. Graphics were generated using Excel and Mathematica (version 11.1.1; Woolfram Research Inc., Champaign, IL, USA). Data analysis was performed using the Real Statistics Resource Pack software (Release 6.8; Copyright [2013–2020] Charles Zaiontz www.real-statistics.com).

Results

All participants invited to take part in the study did so and were able to comprehend the nature of the test and follow the technician's instructions.

The numbers and proportions of participants detecting/identifying one or more of the 14 geometric stimuli, and identifying one or more of the optotypes, are given in Table 2.

Stimulus-Specific Responses

The stimulus-specific responses describe the collective responses of the sample populations to each stimulus.

The stimulus responses were pattern-dependent, with the kinetic and radially symmetric patterns being most salient (Fig. 2A). For all geometric patterns, and for the healthy and three single-condition diagnostic groups (pseudophakia, cataract, and AMD; see Fig. 2A), fewer individuals were able to identify the images than simply detect them. The largest differences between identification and detection scores were recorded for the HB (uniform field) stimuli (#01, alternating HB and #07, static HB). The radially symmetric stimuli (#8, radial; #11, circles; and #13, windmill) were the most readily identified.

Positive optotype identification showed a graded response for the criterion of letter identification (Fig. 2B) for each logMAR value and within each logMAR banding. Compared with geometric patterns, optotypes were less well identified. Within each logMAR banding, the most readily identified letter was Z or N. Responses from the pseudophakic group were similar to those of the healthy group, whereas the cataract and AMD groups performed poorly.

Pattern stimulus response frequencies differed between diagnostic groups. They also differed for the criteria of detection and identification, as demonstrated by the ORs for each diagnostic group (Fig. 3). All diagnostic groups were significantly different from the healthy group (Cochran–Mantel–Haenszel test for multiple contingency tables, $P < 0.001$, see Supple-

Table 2. Pattern Detection, Pattern Identification, and Optotype Identification

		Pattern Detection		Pattern Identification		Optotype Identification	
	n	*n*	%	*n*	%	*n*	%
Normal	47	46	97.9	41	87.2	17	36.2
Pseudophakia	47	42	89.4	40	85.1	17	36.2
Cataract	80	65	81.3	41	51.3	3	3.8
AMD	59	30	50.8	14	23.7	1	1.7
AMD + pseudophakia	57	32	56.1	21	36.8	6	10.5
AMD + cataract	42	21	50.0	7	16.7	0	0.0

Number (*n*) and proportion (%) of participants detecting/identifying one or more stimuli (geometric pattern, optotype).

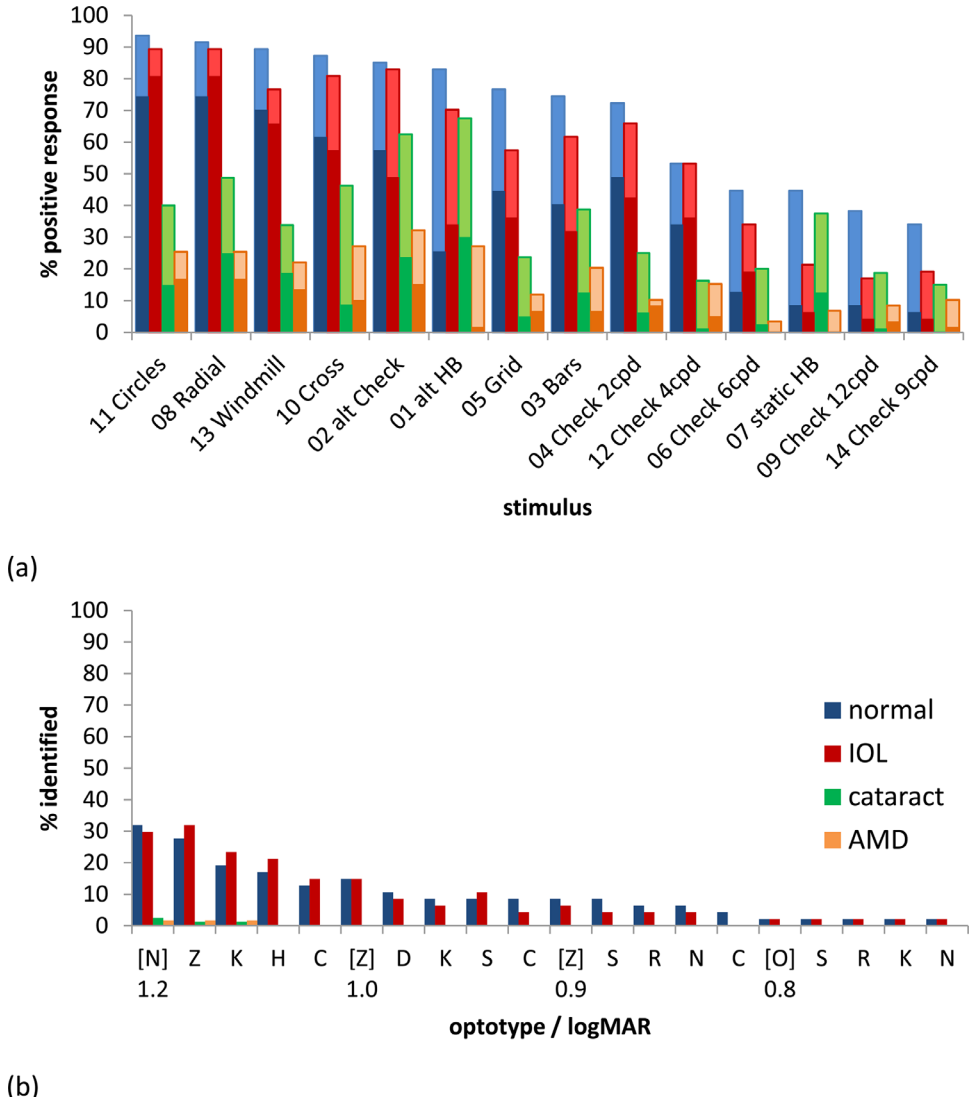

Figure 2. Percentage of positive polarization stimulus responses for healthy (blue), pseudophakic (IOL, red), cataract (green), and AMD (orange) categories. (**A**) Pattern identification (height of darker shaded columns) is superimposed on pattern detection (total height of columns). (**B**) Percentage of optotypes identified. The abscissa shows the optotypes in groups of five, with corresponding logMAR values of 1.2, 1.0, 0.9, and 0.8. Square brackets demarcate the boundary of each logMAR banding.

mentary Material for data and details of analyses). For the criterion of pattern detection, the pseudophakic group had an overall combined OR of 1.73 (95% confidence interval [CI] = 1.39–1.73), and was the closest to healthy compared with the cataract (OR = 4.88, 95% CI = 4.69–6.96) and AMD groups (OR = 13.94, 95% CI = 10.56–17.7). Woolf's test of homogeneity was not significant for the pseudophakic group (W = 13.06, $P = 0.44$), but was significant for the cataract (W = 57.44, $P < 0.001$) and AMD groups (W = 57.44, $P < 0.001$). These results indicate that the variation in responses of the pseudophakic group, but not the cataract and AMD groups, was similar to the healthy group. The same general pattern of results was obtained for the criterion of pattern identification (see Supplementary Material Table S3).

Although the radially symmetric static patterns (#11, circles; #13, windmill; and #8, radial) were most frequently detected and identified by healthy and pseudophakic subjects, the kinetic uniform field (#01) and kinetic checkerboard (#02) patterns were the most frequently detected/identified in the cataract and AMD groups. Although the AMD group responses were depressed in comparison with the other groups, they followed the same pattern of responses as the cataract group (see Fig. 3).

The ORs for individual stimuli in each patient category are presented in detail in Supplementary

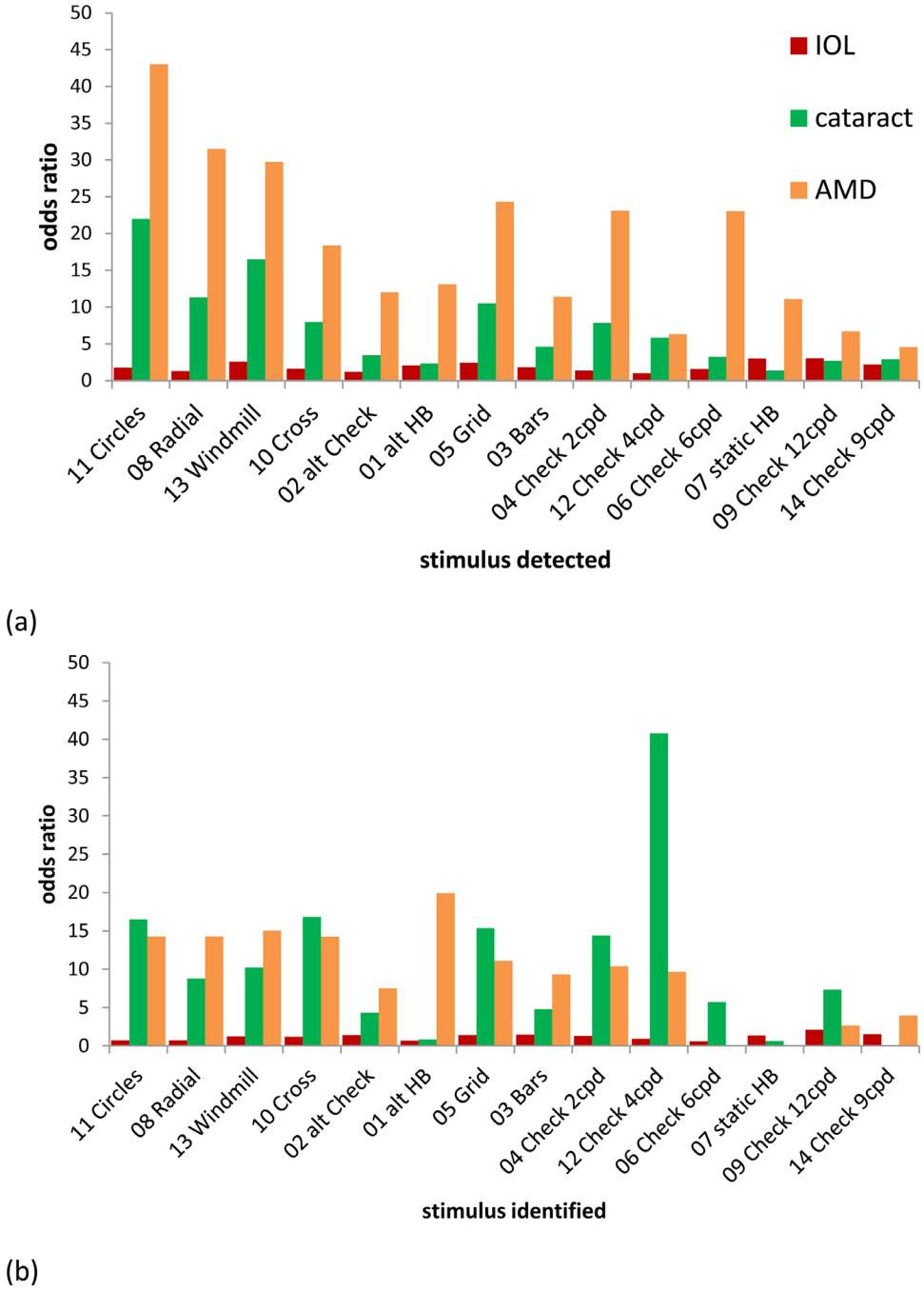

Figure 3. Odds ratios for pseudophakic (IOL, red), cataract (green), and AMD (orange) categories. Results are shown for the criterion of (**A**) pattern detection and (**B**) pattern identification.

Material Tables S2 and S3, and summarized in Figure 3. For pattern detection, the trend in positive patient responses, compared with the healthy group, was consistent across all test stimuli: responses were greatest in subjects with pseudophakia, intermediate in the cataract group, and least in the AMD group. Note that the high OR for pattern identification of stimulus #12 (4 cpd check; Fig. 3B) is for one value only (Supplementary Material Table S3).

Participant-Specific Responses: Group Total *Ps* Score for Diagnostic Categories

Here, the responses of individuals from each sample population are presented in terms of the *Ps* score metric.

In total, there were six diagnostic categories: healthy, AMD, cataract, pseudophakia, cataract and AMD, and pseudophakia and AMD. For each category, a

Table 3. Summary *Ps* Score Data for the Six Diagnostic Categories, Together With *P* Values Derived From the Mann-Whitney *U* Test for Two Independent Samples (Two-Tailed)

	Healthy	AMD	Cataract	Pseudophakia	AMD + Cataract	AMD + Pseudophakia
N	47	59	80	47	42	57
Minimum	0	0	0	0	0	0
Maximum	61	23	22	85	16	75
Median	17	1	6	13	0.5	1
Mode	17	0	0	13	0	0
Mann-Whitney *P* values		AMD	Cataract	Pseudophakia	AMD + Cataract	AMD + Pseudophakia
	Healthy	0.00	0.00	0.32	0.00	0.00
	AMD		0.00	0.00	0.79	0.22
	Cataract			0.00	0.00	0.02
	Pseudophakia				0.00	0.00
	AMD + cataract					0.15

summary of the *Ps* score data and comparative statistics (two-tailed Mann-Whitney *U* test) is presented in Table 3, with associated frequency histograms presented in Figure 4.

An overall Kruskal-Wallace analysis of the six groups revealed a significant difference among groups ($H = 115.17$, $P < 0.001$). For paired comparisons (Mann-Whitney test with and without Bonferroni

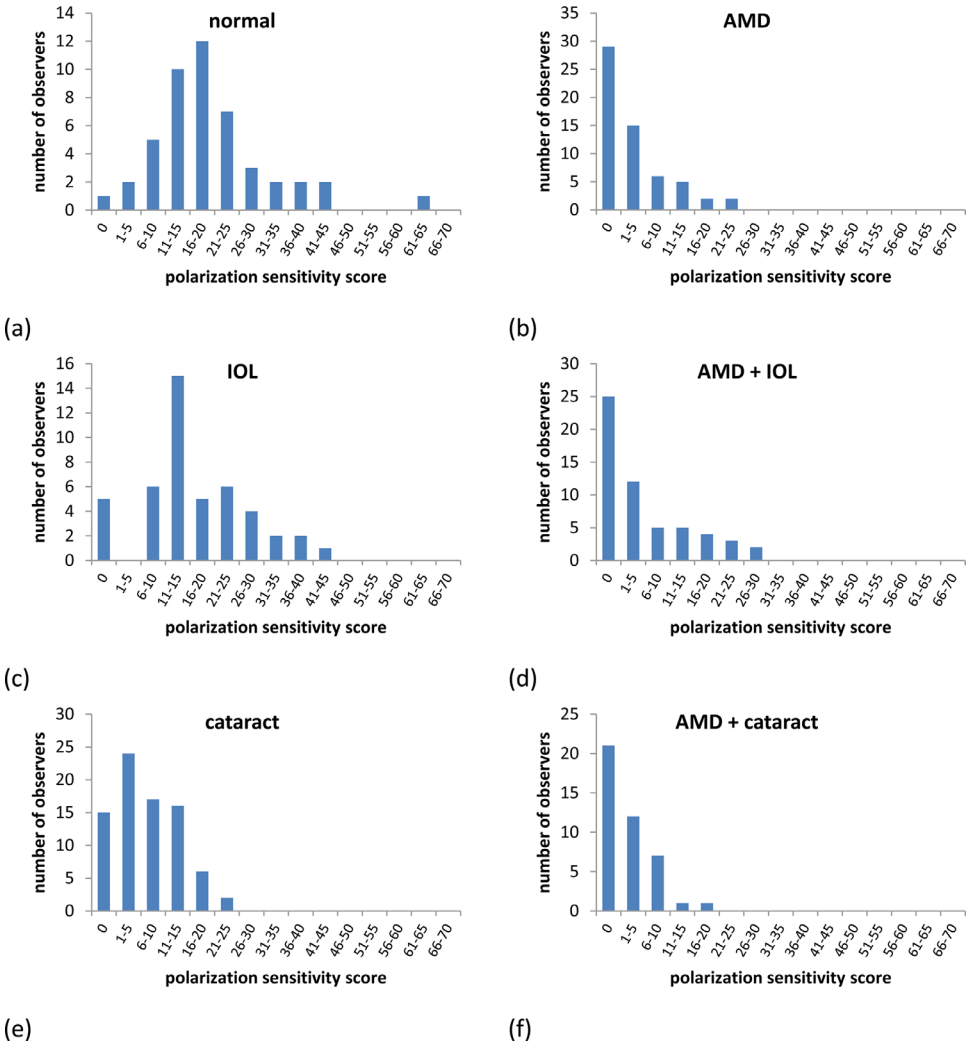

Figure 4. Polarization sensitivity score (*Ps*) for: (**A**) healthy eyes ($n = 47$); (**B**) eyes with macular degeneration ($n = 59$); (**C**) pseudophakic eyes with no co-pathology (IOL, $n = 47$); (**D**) pseudophakic eyes with AMD (AMD + IOL, $n = 57$); (**E**) eyes with cataracts ($n = 80$); and (**F**) eyes with both cataract and macular degeneration ($n = 42$).

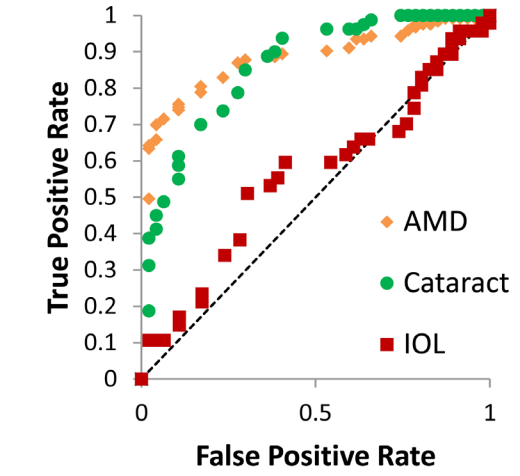

(a)

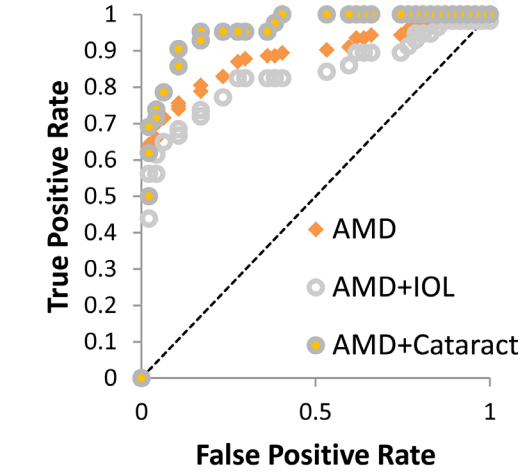

(b)

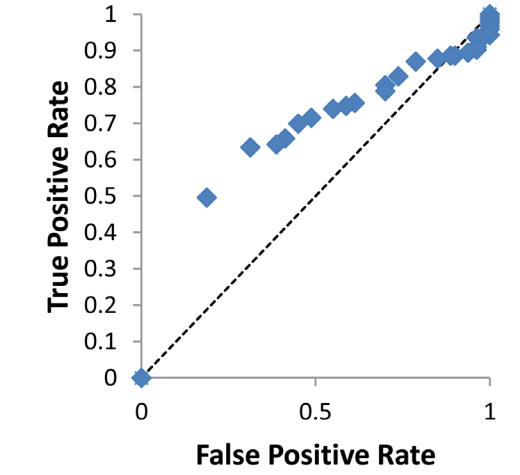

(c)

Figure 5. Receiver operating characteristic (ROC) curves for *Ps* score of clinical groups compared with the healthy cohort and (**A**) AMD, cataract, pseudophakia (IOL) groups; and (**B**) AMD, AMD + Pseudophakia (AMD + IOL), and AMD + cataract groups. (**C**) AMD group compared with cataract group. The dotted line in panels **A** and **B** indicates equivalence to the healthy group; the dotted line in panel **C** indicates equivalence of the AMD and cataract groups (AUC = 0.5).

correction), there was no significant difference ($P > 0.05$) between the healthy and pseudophakia groups, or among the three AMD groups (see Figs. 4B, 4D, 4F). However, there were significant differences ($P < 0.001$) among each of the three AMD groups and both the healthy (see Fig. 4A) and pseudophakia groups. There were also significant differences ($P < 0.05$) between the cataract group and all other groups (see Fig. 4E).

The *Ps* score was evaluated by ROC curve analysis (Fig. 5), in which the total AUROC was taken as an index of the predictive value in differentiating the diagnostic group in question from the healthy group. For pseudophakia (see Fig. 5A), *Ps* was not significantly different from the healthy eyes (AUROC = 0.57, 95% CI = 0.46–0.57), and may therefore have little predictive value for this diagnostic group. However, the predictive value of *Ps* in differentiating cataract from healthy eyes was high (AUROC = 0.87, 95% CI = 0.81–0.89).

For AMD alone (see Figs. 5A, 5B), the predictive value of *Ps* was high and significant (AUROC = 0.89, 95% CI = 0.84–0.91). The AUROC in eyes with AMD was increased by the presence of cataract (AUROC = 0.96, 95% CI = 0.91–0.98; Fig. 5C), and reduced by pseudophakia (AUROC = 0.84, 95% CI = 0.77–0.86). The ROC curves for cataract and AMD alone were different (see Fig. 5A) and, comparing the two groups (see Fig. 5C), the AUROC was significantly greater than 0.5 (AUROC = 0.72, 95% CI = 0.65–0.72).

Relationship Between *Ps* Score and Visual Acuity

There was no linear correlation of *Ps* with visual acuity for any of the diagnostic groups (Pearson product moment R^2 healthy 0.03, cataract 0.04, AMD 0.07, all groups combined 0.1).

Plots of normalized frequencies of *Ps* scores (intervals of 5), relative to logMAR visual acuity (intervals of 0.2), are shown in Figure 6 for the healthy, cataract, and AMD diagnostic groups. The response values for healthy eyes (see Fig. 6A) were clustered between logMAR 0–0.4 and *Ps* of 10–30. Note that the response cluster moves progressively down and to the right for cataracts (logMAR = 0.2–0.6, *Ps* score = 5–15; Fig. 6B) and AMD (logMAR = 0.2–0.8, *Ps* score = 0–10; see Fig. 6C). This analysis suggests

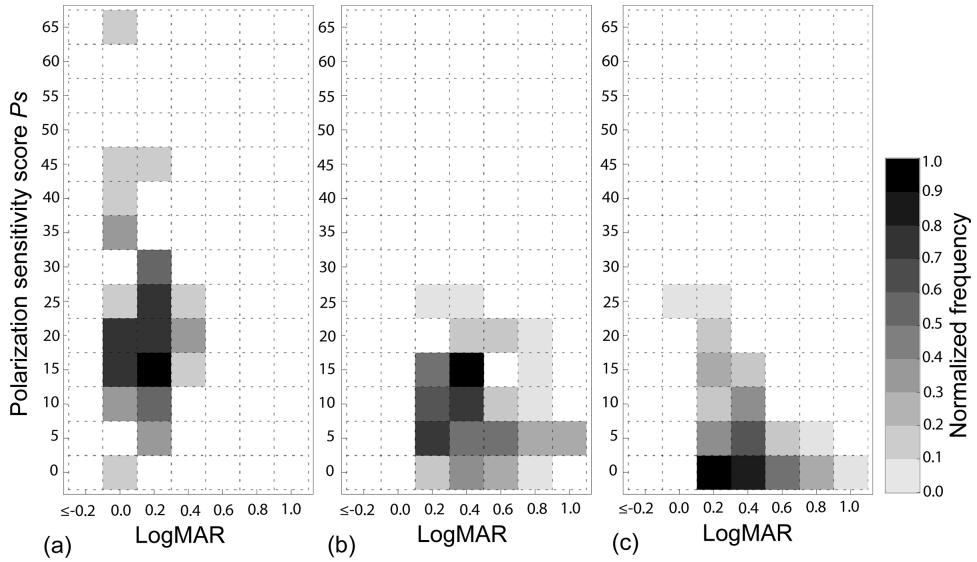

Figure 6. Density plot of normalized frequency (greyscale) of polarization sensitivity scores (*Ps*, vertical axis, intervals of 0, 1–5, 6–10, etc.) and logMAR visual acuity (horizontal axis, intervals of 0.2) for: (**A**) healthy; (**B**) cataract; and (**C**) AMD diagnostic groups.

that the ratio of polarization sensitivity score to logMAR visual acuity (*Ps*/VA) changes with condition. The *Ps*/VA ratio was significantly different for the overall comparison among groups (H = 8.37; $P = 0.02$). Furthermore, healthy, AMD, and cataract eyes were all different from each other (healthy/cataract: U = 636, $P = 0.02$; healthy/AMD: U = 862, $P = 0.04$; and cataract/AMD: U = 1071, $P = 0.045$).

Discussion

Sensitivity measures of polarization-modulated stimuli have the potential to provide a highly targeted means by which to assess macular function in health and disease,[1,3,11,13,18] a fact that has been recognized for some time.[9,12] Currently, however, such measures are rarely if ever used in daily clinical practice. This is principally because a rigorous quantitative measure of human vision with polarization targets has not been available, and because of the difficulty in generating such patterns. Here, using existing LCD technology, we demonstrated the use of an inexpensive, compact means by which to assess macular function in a naïve clinical population. In doing so, we show for the first time that polarization-modulated patterns are effective in distinguishing AMD from healthy maculae (see Figs. 4, 5). Importantly, this conclusion was not based solely on sensitivity measures to a single visual target, but rather to a formulated battery of stimuli that provided a graded response measure, termed the *Ps* score. The acceptance and satisfactory performance by all participants indicate that this novel metric is applicable to a clinic setting with naïve individuals.

Effect of Media Opacities

Because AMD and cataract frequently co-exist, it was necessary to assess the effect of each and both combined on polarization perception.

It has previously been supposed that, in the presence of intact macular function and a visual acuity better than logMAR 1.0, perception of HB generated by a uniform polarization stimulus is relatively insensitive to media opacities.[9,12] This is supported by our findings for the alternating HB stimulus (#01 alt HB; see Fig. 1A), where the frequencies of both detection and identification of the phenomenon are similar in the healthy, pseudophakic, and cataract groups. This result is also reflected in the reported ORs for individual stimuli in each patient category (see Supplementary Material Tables S2 and S3, Fig. 3). The proposition that the perception of HB in the presence of cataracts is a good indicator of macular function[12] is therefore upheld, and we demonstrate the utility of a liquid-crystal-based means of generating this phenomenon suitable for clinical practice.

Unlike HB, polarization modulated patterns contain high spatial frequency components associated with edge contours, and as such are susceptible to image blurring and possibly depolarization by intraocular light scatter from media opacities. It is therefore not surprising that, compared with healthy eyes, the

cataract group demonstrated reduced polarization pattern sensitivity. This result was evident in both the responses of individuals to stimuli of different saliencies (see Figs. 2, 3), and in the values of the devised polarization sensitivity metric (Figs. 4, 5).

Effects of Intraocular Lens Implants

With current surgery rates for cataracts (e.g. approximately 0.45 M cases per year in the United Kingdom), pseudophakia is common in individuals over the age of 65 years, with at least 10% of cataract extractions performed on individuals with AMD.[19] Polymer materials used for intraocular lens optics are potentially birefringent and might therefore alter the state of polarization incident on the macula, compromising PPP measurements. An early laboratory study of intraocular lens optics did not report any appreciable birefringence in the lenses tested.[20] This is supported by our findings (see Supplementary Material) that no measurable birefringence was evident in samples of intraocular lens types identified in the pseudophakic group. The finding that pseudophakia did not degrade PPP (Figs. 4, 5) has wider importance, as it implies that pseudophakia does not affect the state of polarized light transmitted through ocular media, and that the presence of an intraocular lens will not interfere with polarization-sensitive investigations (e.g. OCT technology).

Utility of Different Polarization-Modulated Targets

Different polarization patterns have different saliencies, both in ophthalmologically healthy and unhealthy individuals (Figs. 2–4). Full-field, radially symmetric patterns (e.g. concentric circles [#11] and radial "star-burst" [#08]) have higher detection and identification rates than uniform field HB stimuli (#01, #07). Optotype stimuli, which are discrete and limited to a small area of visual field, are the least well perceived. The OR data (see Fig. 3) suggests that the radially symmetric patterns, at least for the criterion of pattern detection, are most affected by AMD. Such stimuli might therefore have benefits over conventional methods of self-assessment (e.g. Amsler grid) for monitoring the progression of macular disease.

The positive responses for both the healthy and unhealthy groups to the rectilinear stimuli (checkerboard, grating [#03] and grid patterns [#05]) were dependent on their fundamental spatial frequency (see Figs. 2A, 3). This is compatible with a previous finding[13] that the positive response rates of healthy individuals to checkerboard stimuli are proportional to the logarithm of their fundamental spatial frequency. These findings imply that appropriate stimuli could be designed to quantify a range of polarization sensitivity in eyes with both normal and abnormal visual function.

There is no linear correlation between VA and PPP, suggesting that both variables act independently. When comparing visual acuity with *Ps* scores (see Fig. 5), the data points for the healthy group have low logMAR values (normal visual acuity) and variable, high *Ps* scores (i.e. align with the y-axis; see Fig. 5), whereas those for the AMD group have variable, high logMAR values (low visual acuity) and low *Ps* scores (i.e. align with the x-axis; see Fig. 5). The data points for the cataract group fall in between the data clusters for the healthy and AMD patient groups. In brief, visual acuity and PPP metrics give complementary information that, in combination, might be of diagnostic value in assessing macular function. This is supported by the significant differences found between diagnostic groups for the *Ps*/VA ratio, and may form the basis for a more complex metric, including additional quantifiers of macular structure and function.

Conclusions

In the absence of significant cataract, or in the presence of pseudophakia, the extent by which PPP is degraded by AMD supports its possible use in the assessment of this condition and other disorders that affect the macula, such as diabetic retinopathy. Importantly, we make this determination on the clinical utility of PPP based on the responses to a battery of stimuli of differing visual salience, represented as a single metric. Whereas the Amsler Chart remains in frequent use in daily clinical practice, its inaccuracy,[21] and the need for early detection or progression of macular disease,[22] has led to the search for simple and inexpensive replacements. Given the global presence of macular disease, including within many health care environments with limited resources, the use of PPP in assessing macular function, possibly combined with other simple metrics of visual function, may be expedient as the technology required to generate the stimuli is simple, compact, inexpensive, and readily available.

Acknowledgments

The authors thank the following: Alison Marriot (Departmental Manager, Warwick Hospital) and Sara Queen (Clinical Director, Eye Clinic, Warwick Hospital) for administrative and clinical assistance; Mark

Dunne (Aston University, UK) for assistance with statistical analyses; and Shelby E Temple for critical review of the manuscript.

G.P.M. is partly funded by a grant from the European Society of Cataract and Refractive Surgeons.

Author Contributions: G.P.M. conceived the idea, built the equipment, designed the experiments, conducted the data analysis, wrote the paper, and was the project administrator. S.J.A. did the psychophysical analysis, designed the experiments, conducted the data analysis, and wrote the paper. R.A.A. gathered the statistics, conducted the data analysis, and reviewed the paper. M.G. conducted the data acquisition, conducted the database management, and reviewed the paper. D.R. conducted the data acquisition, conducted the database management, and reviewed the paper.

Disclosure: **G.P. Misson**, None; **S.J. Anderson**, None; **R.A. Armstrong**, None; **M. Gilett**, None; **D. Reynolds**, None

References

1. Misson GP, Timmerman BH, Bryanston-Cross PJ. Human perception of visual stimuli modulated by direction of linear polarization. *Vision Res*. 2015;115(Part A):48–57.
2. Temple SE, McGregor JE, Miles C, et al. Perceiving polarization with the naked eye: characterization of human polarization sensitivity. *Proc R Soc B*. 2015;282:20150338.
3. Misson GP, Anderson SJ. The spectral, spatial and contrast sensitivity of human polarization pattern perception. *Sci Rep*. 2017;7:16571.
4. Naylor EJ, Stanworth A. Retinal pigment and the Haidinger effect. *J Physiol*. 1954;124:543–552.
5. Bone RA. The role of the macular pigment in the detection of polarized light. *Vision Res*. 1980;20:213–220.
6. McGregor J, Temple SE, Horváth G. Human Polarization Sensitivity. In: Horváth G (ed), *Polarized Light and Polarization Vision in Animal Sciences.* Heidelberg, Germany: Springer; 2014:303–315.
7. Misson GP, Temple SE, Anderson SJ. Computational simulation of Haidinger's brushes. *J Opt Soc Am A*. 2018;35:946–952.
8. Goldschmidt M. A new test for function of the macula lutea. *Arch Ophthalmol*. 1950;44:129–135.
9. Forster HW. The Clinical Use of the Haidinger's Brushes Phenomenon. *Am J Ophthalmol*. 1954;38:661–665.
10. Sloan LL, Naquin HA. A Quantitative Test for Determining the Visibility of the Haidinger Brushes: Clinical Applications. *Am J Ophthalmol*. 1955;40:393–406.
11. Muller PL, Muller S, Gliem M, et al. Perception of Haidinger Brushes in Macular Disease Depends on Macular Pigment Density and Visual Acuity. *Invest Ophthalmol Vis Sci*. 2016;57:1448–1456.
12. Stanworth A, Naylor EJ. The measurement and clinical significance of the Haidinger effect. *Trans Ophthalmol Soc UK*. 1955;75:67–79.
13. Misson GP, Anderson SJ, Armstrong RA, Gillett M, Reynolds D. The Clinical Application of Polarization Pattern Perception. *Transl Vis Sci Technol*. 2020;9:31.
14. Klein BEK, Howard KP, Lee KE, Iyengar SK, Sivakumaran TA, Klein R. The Relationship of Cataract and Cataract Extraction to Age-related Macular Degeneration: The Beaver Dam Eye Study. *Ophthalmology*. 2012;119:1628–1633.
15. Kessel L, Erngaard D, Flesner P, Andresen J, Tendal B, Hjortdal J. Cataract surgery and age-related macular degeneration. An evidence-based update. *Acta Ophthalmologica*. 2015;93:593–600.
16. Davis MD, Gangnon RE, Lee LY, et al. The Age-Related Eye Disease Study severity scale for age-related macular degeneration: AREDS Report No. 17. *Arch Ophthalmol*. 2005;123:1484–1498.
17. Foster JJ, Temple SE, How MJ, et al. Polarisation vision: overcoming challenges of working with a property of light we barely see. *Naturwissenschaften*. 2018;105:27.
18. Temple SE, Roberts NW, Misson GP. Haidinger's brushes elicited at varying degrees of polarization rapidly and easily assesses total macular pigmentation. *J Opt Soc Am A*. 2019;36:B123–B131.
19. Royal College of Ophthalmologists UK. National Ophthalmology Database Audit Annual Report. *NOD Audit Annual Reports: Royal College of Ophthalmologists*; 2020, Available at: https://www.nodaudit.org.uk.
20. Miura M, Osako M, Elsner AE, Kajizuka H, Yamada K, Usui M. Birefringence of intraocular lenses. *J Cataract Refract Surg*. 2004;30:1549–1555.
21. Schuchard RA. Validity and Interpretation of Amsler Grid Reports. *Arch Ophthalmol*. 1993;111:776–780.
22. Crossland M, Rubin G. The Amsler chart: absence of evidence is not evidence of absence. *Br J Ophthalmol*. 2007;91:391.